Reactions of Laser-Ablated Be and Mg Atoms with C_2H_2: Infrared Spectra and Density Functional Calculations of Novel Metal−Acetylene Species

Craig A. Thompson and Lester Andrews*

Contribution from the Department of Chemistry, University of Virginia, Charlottesville, Virginia 22901

Received May 20, 1996[⊗]

Abstract: Reactions of laser-ablated Be and Mg atoms with C_2H_2, $^{13}C_2H_2$, and C_2D_2 upon condensation in excess argon at 10 K give new infrared absorptions that are assigned to the insertion and decomposition products HBeCCH, BeCCH, and MgCCH with the help of density functional theory isotopic frequency calculations. The 2019-cm^{-1} C≡C stretching fundamental for BeCCH is between values for BCCH and AlCCH, which are all slightly blue shifted from acetylene itself.

Introduction

The reaction of metal atoms with small hydrocarbon molecules is an active field of research.[1−13] Such studies are important for understanding catalysis and chemisorption as well as for developing new synthetic methods. Recent studies have shown that thermal aluminum atoms react with acetylene to give new addition products;[7] however, laser-ablated aluminum and boron atoms react with acetylene to produce new insertion and decomposition products, namely AlCCH, HBCCH, and BCCH.[8,9] It is of interest to note that thermal Ca and Sr atoms react directly with acetylene to give CaCCH and SrCCH[10] and laser ablated Mg reacts with methane in a supersonic expansion to give the MgCCH molecule.[11] However, thermally evaporated Li atoms form an addition product, LiC_2H_2 (C_{2v}),[12] while Na atoms form an acetylene complex that rearranges on photolysis ($\lambda > 5000$ Å) to a vinylidene complex, $NaCCH_2$.[13]

Reactions of laser-ablated beryllium atoms with O_2, H_2, N_2, and H_2O have produced novel chemical species such as OBeO, ArBeO, HBeH, NNBeNN, and HOBeOH.[14−17] No experimental reactions of beryllium with acetylene have been reported; however, a number of theoretical investigations of the Be−C_2H_2 interaction have appeared.[18−20] Flores and Largo have calculated the most stable structure to be the linear HBeCCH insertion product.[20] Studies by Breckenridge and Unemoto on collisional quenching of electronically excited Mg indicate that Mg (3s 3p, $^1P_1$) reacts with H_2, CH_4, C_3H_6, and C_3H_8 to produce MgH but not with C_2H_4 and C_2H_2.[21] In contrast, spectra reported here show that laser-ablated beryllium and magnesium atoms react with acetylene to form new product molecules, as well as BeH and MgH.

Experimental Section

The apparatus for pulsed-laser ablation matrix-isolation spectroscopy has been described earlier.[22,23] Reagent grade acetylene (Matheson), $^{13}C_2H_2$ (92% ^{13}C), and C_2D_2 (98% D, Merck Sharp and Dohme) were all purified by pumping on condensed samples prior to thawing for dilution with argon (99.995%, Air Products) to make gas samples. Beryllium metal (Johnson-Matthey) and magnesium (^{n}Mg rod; Fisher; ^{26}Mg, 96%, Oak Ridge National Laboratory) were used. Briefly, Ar: C_2H_2 mixtures ranging from 200:1 to 400:1 were codeposited at 2 mmol/h onto a 10 ± 1 K substrate with metal atoms ablated using a Nd:YAG laser (1064 nm) focused (10 cm focal length) onto a rotating metal target with laser energies ranging from 40 to 80 mJ/pulse at the target. Infrared spectra were recorded at 0.5 cm^{-1} resolution and ±0.1 cm^{-1} accuracy on a Nicolet 750 FTIR using a liquid N_2 cooled MCT detector. The samples were subjected to mercury arc photolysis (Philips 175 W) and annealing cycles and more spectra were recorded.

Results

Product bands were grouped based on varying yields in separate experiments as well as band profiles. Bands are labeled with their assignments to simplify nomenclature.

Be + C_2H_2. The codeposition of laser-ablated Be and C_2H_2 in excess argon produced a weak new band at 3325.9 cm^{-1} in

---

[⊗] Abstract published in *Advance ACS Abstracts*, September 15, 1996.

(1) Klabunde, K. J.; Tanaka, Y. *J. Am. Chem. Soc.* **1983**, *105*, 3544.

(2) Chenier, J. M. B.; Howard, J. A.; Mile, B.; Sutcliffe, R. *J. Am. Chem. Soc.* **1983**, *105*, 788. Kasai, P. H. *J. Am. Chem. Soc.* **1983**, *105*, 6704.

(3) Kafafi, Z. H.; Hauge, R. H.; Margrave, J. L. *J. Am. Chem. Soc.* **1985**, *107*, 7550.

(4) Brown, S. H.; Crabtree, R. H. *Chem. Commun.* **1987**, 970.

(5) *Selective Hydrocarbon Activation*; Davies, J. A., Watson, P. L., Greenberg, A., Liebman, J. F., Eds.; VCH Publishers, Inc.: New York, 1990.

(6) Greene, T. M.; Andrews, L.; Downs, A. J. *J. Am. Chem. Soc.* **1995**, *117*, 8180.

(7) Burkholder, T. R.; Andrews, L. *Inorg. Chem.* **1993**, *32*, 2491.

(8) Chertihin, G. V.; Andrews, L.; Taylor, P. R. *J. Am. Chem. Soc.* **1994,** *116*, 3513.

(9) Andrews, L.; Hassanzadeh, P.; Martin, J. M. L.; Taylor, P. *J. Phys. Chem.* **1993**, *97*, 5839.

(10) (a) Bopegedera, A. M. R. P.; Brazier, C. R.; Bernath, P. F. *Chem. Phys. Lett.* **1987**, *136*, 97. Bopegedera, A. M. R. P.; Brazier, C. R.; Bernath, P. F. *J. Mol. Spectrosc.* **1988**, *129*, 268. (b) Whitham, C. J.; Soep, B.; Visticot, J.-P.; Keller, A. *J. Chem. Phys.* **1990**, *93*, 991.

(11) (a) Anderson, M. A.; Ziurys, L. M. *Astrophys. J.* **1995**, *439*, L25. (b) Corlett, G. K.; Little, A. M.; Ellis, A. M. *Chem. Phys. Letts.* **1996**, *249*, 53. (c) Ellis, A. M. Personal communication.

(12) Manceron, L.; Andrews, L. *J. Am. Chem. Soc.* **1983**, *107*, 563.

(13) Kasai, P. H.; McLeod, D.; Watanabe, T. *J. Am. Chem. Soc.* **1977**, *99*, 3521. Kassai, P. H. *J. Phys. Chem.* **1982**, *86*, 4092.

(14) Thompson, C. A.; Andrews, L. *J. Chem. Phys.* **1994**, *100*, 8689.

(15) Tague, T. J., Jr.; Andrews, L. *J. Am. Chem. Soc.* **1993**, *115*, 12111.

(16) Thompson, C. A.; Andrews, L.; Davy, R. D. *J. Phys. Chem.* **1995**, *99*, 7913.

(17) Thompson, C. A.; Andrews, L. *J. Phys. Chem.* In press.

(18) (a) Swope, W. C.; Schaefer, H. F. *J. Am. Chem. Soc.* **1976**, *98*, 7962. (b) Witko, M.; Bonacic-Koutecky, V. *J. Quantum Chem.* **1986**, *29*, 1535.

(19) (a) Sakai, S.; Morokuma, K. *J. Phys. Chem.* **1987**, *91*, 3661; (b) Balaji, V.; Jordan, K. D. *J. Phys. Chem.* **1988**, *92*, 3101.

(20) Flores, J. R.; Largo, A. *J. Phys. Chem.* **1991**, *95*, 9278.

(21) Breckenridge, W. H.; Unemoto, H. *J. Chem. Phys.* **1981**, *75*, 698.

(22) Burkholder, T. R.; Andrews, L. *J. Chem. Phys.* **1991**, *95*, 8697. Andrews, L.; Burkholder, T. R. *J. Phys. Chem.* **1991**, *95*, 8554.

(23) Hassanzadeh, P.; Andrews, L. *J. Phys. Chem.* **1992**, *96*, 9177.

S0002-7863(96)01684-8 CCC: $12.00

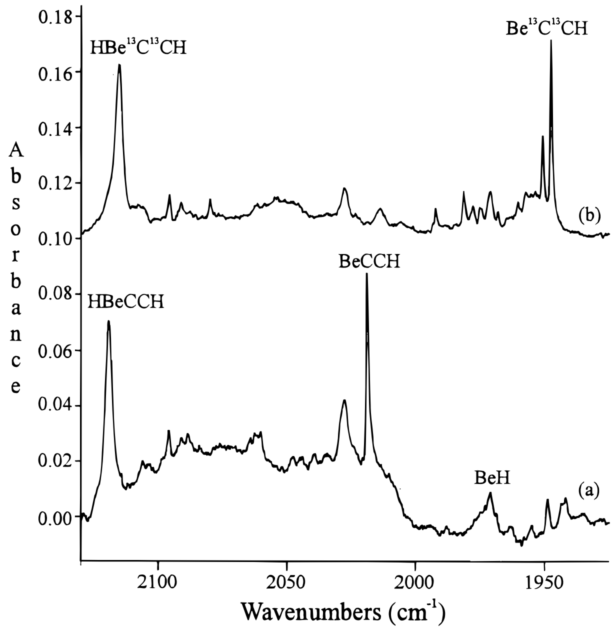

Figure 1. Infrared spectra from 2135 to 1925 cm^{-1} for Be + C_2H_2 reaction products in solid argon at 10 ± 1 K: (a) Be + C_2H_2, and (b) Be + $^{13}C_2H_2$. Codeposition of Be, 70 mJ/pulse, and Ar/C_2H_2 = 200/1 samples for 2 h.

addition to the strong acetylene bands at 3301.9 and 3288.9 cm^{-1}.[24] The former band, not present in Ar/C_2H_2 blank samples, is a reaction product, diacetylene,[25] in laser-ablation experiments. The spectrum in the region expected for C−C and Be−H stretching vibrations is shown in Figure 1a for Be + C_2H_2 in excess argon. A strong band at 2119.4 cm^{-1} marked HBeCCH is accompanied by a sharp band at 2018.9 cm^{-1} marked BeCCH. Weak BeH_2 and BeH bands were present at 2159.4 and 1970.1 cm^{-1}.[15] In addition the CCH radical band was observed at 1845.8 cm^{-1}.[26-28] Frequencies for product absorptions are listed in Table 1. With the exception of weak beryllium oxide[14] and nitride[16] bands from trace air contaminant, no product absorptions were observed between 2000 and 900 cm^{-1}.

The spectrum for the same Be + C_2H_2 experiment is shown in Figure 2a in the region expected for Be−C stretching modes and CCH bending modes. A sharp band at 866.3 cm^{-1} is due to the strongest absorption of $(BeO)_2$.[14] Sharp bands at 855.0 and 838.9 cm^{-1} are marked BeCCH and HBeCCH, respectively. Two intense bands at 744.9 and 736.7 cm^{-1} due to C_2H_2 dimer and monomer, respectively, are truncated to show weaker product bands. The sharp band at 696.8 cm^{-1} is due to the bending mode of BeH_2.[15] A broad band at 689.1 cm^{-1} and a sharper band at 675.7 cm^{-1} are marked HBeCCH and BeCCH, respectively. The lower region in Figure 3a reveals a sharp doublet at 553.0 and 550.0 cm^{-1} also marked HBeCCH. A weak band at 628.1 cm^{-1} (not shown) is due to diacetylene.[25]

Photolysis of samples had no effect on product bands. Annealing to temperatures ranging from 20 to 30 K decreased band intensities from 10 to 25%; however, all bands decreased comparable amounts and selective reactions were not observed.

Be + $^{13}C_2H_2$. Experiments with $^{13}C_2H_2$ were carried out to assist in the identification of product molecules. As expected, $^{13}C_2H_2$ bands at 3284.7 and 3270.7 cm^{-1} were observed in the C−H stretching region along with $^{13}C_4H_2$ at 3308.9 cm^{-1}.

Table 1. Absorptions (cm^{-1}) Observed for Be + HCCH Reaction Products in Solid Argon

				$^{12}C/^{13}C$ ratios	
assign	HCCH	$H^{13}C^{13}CH$	DCCD	obsd	calcd[a]
HCCCCH	3325.9	3308.9	2593	1.005 138	
BeH_2	2159.4	2159.4	1674.3		
HBeCCH	2119.4	2115.2	1535.0	1.001 986	1.003 02
BeCCH	2018.9	1947.8	1873.4	1.003 650	1.036 94
BeH	1970.1	1970.1	1477.6		
CCH	1845.8	1785.5	1746.9	1.033 772	1.036 736
BeCCH	855.0[b]	846.2	848.9	1.010 399	1.010 012
HBeCCH	838.9[c]	829.6	784.9	1.011 210	1.010 826
C_2H_2	736.7	734.9	542.5	1.002 449	1.003 051
HBeCCH	689.1	683.3		1.008 488	1.009 690
BeCCH	675.7	671.4	553.8	1.006 404	1.009 475
HCCCCH	628.1	624	495.6		
(site)	553.0	551.5	451.3	1.002 720	1.003 414
HBeCCH	550.0	548.4	450.0	1.002 918	1.003 414

[a] Calculated by DFT, Tables 4 and 5. [b] Mixed 12/13 intermediates at 851.8 and 849.0 cm^{-1}. [c] Mixed isotopic intermediate at 833.3 cm^{-1}.

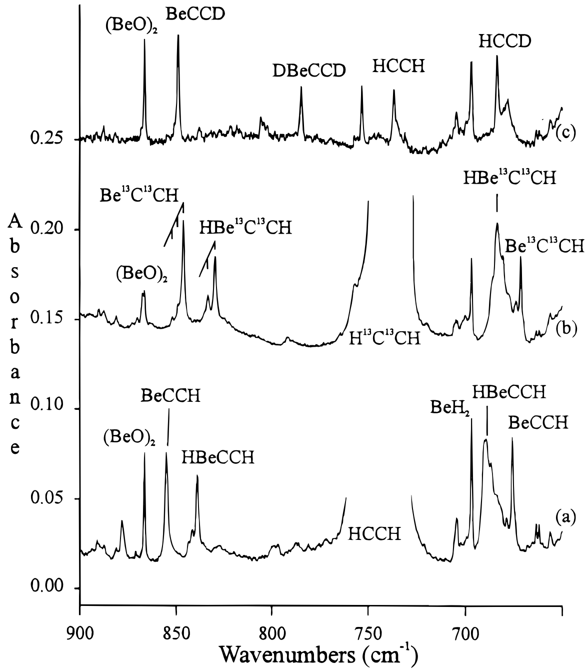

Figure 2. Infrared spectra from 900 to 650 cm^{-1} for Be + C_2H_2 reaction products in solid argon at 10 ± 1 K: (a) Be + C_2H_2, (b) Be + $^{13}C_2H_2$, and (c) Be + C_2D_2, spectrum expanded ×3 relative to the absorbance scale given for spectra a and b. Codeposition of Be, 70 mJ/pulse, and Ar/C_2H_2 = 200/1 samples for 2 h.

The Be + $^{13}C_2H_2$ codeposition spectrum (Figure 1b) shows a strong band at 2115.2 cm^{-1} marked $HBe^{13}C^{13}CH$ shifted only 4.2 cm^{-1} from its ^{12}C counterpart. In contrast, the sharp band at 1947.8 cm^{-1} (marked $Be^{13}C^{13}CH$) shifted significantly in the ^{13}C experiments as did the $^{13}C^{13}CH$ band at 1785.5 cm^{-1}.[26-28] The spectrum (Figure 2b) revealed an isotopic counterpart band at 846.2 cm^{-1} accompanied by weak isotopic intermediate bands at 851.8 and 849.0 cm^{-1} marked with isotope bars. Similarly a sharp band at 829.6 cm^{-1} accompanied by an intermediate band at 833.3 cm^{-1} is marked $HBe^{13}C^{13}CH$. The acetylene bands are again truncated. BeH_2 was observed unshifted along with a broad band at 683.3 cm^{-1}, marked $HBe^{13}C^{13}CH$, and a sharp band at 671.4 cm^{-1}, marked $Be^{13}C^{13}CH$. The spectrum in Figure 3b shows the lowest product absorption with a small ^{13}C shift to 551.5 cm^{-1}.

---

(24) Andrews, L.; Johnson, G. K.; Kelsall, B. J. *J. Phys. Chem.* **1982**, *86*, 3374, 3380.

(25) Patten, K. O.; Andrews, L. *J. Phys. Chem.* **1986**, *90*, 3910.

(26) Jacox, M. E. *Chem. Phys.* **1975**, *7*, 424.

(27) Shepherd, R. A.; Graham, W. R. M. *J. Chem. Phys.* **1987**, *86*, 2600.

(28) Jacox, M. E.; Olson, W. B. *J. Chem. Phys.* **1987**, *86*, 3134.

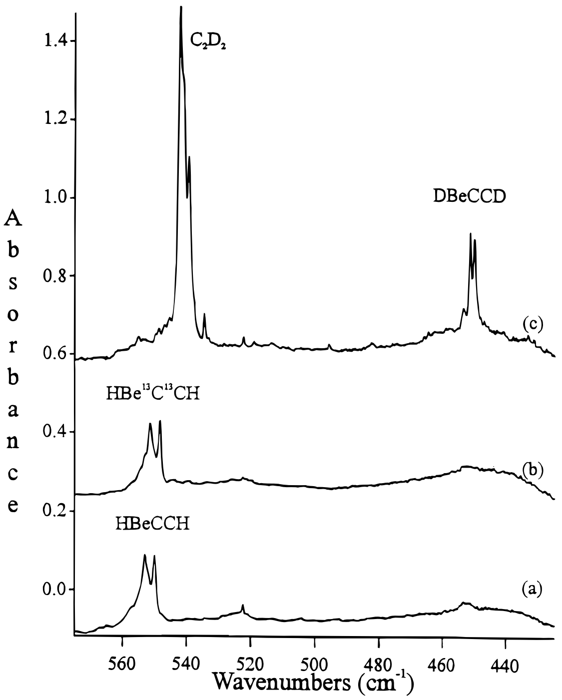

Figure 3. Infrared spectra from 570 to 430 cm^{-1} for Be + C_2H_2 reaction products in solid argon at 10 ± 1 K: (a) Be + C_2H_2, (b) Be + $^{13}C_2H_2$, and (c) Be + C_2D_2. Codeposition of Be, 70 mJ/pulse, and Ar/C_2H_2 = 200/1 samples for 2 h.

Be + C_2D_2. Experiments with deuterated acetylene were also conducted. Absorptions were generally weaker owing to isotope intensity effects. As expected, bands for C_2D_2 were observed at 2441.7 and 2432.8 cm^{-1}. The CCD and BeD_2 products were observed at 1746.9, and 1674.3 cm^{-1}, respectively in agreement with earlier reports.[15,26−28]

A Be + C_2D_2 spectrum is shown in Figure 2c. Note the band at 848.9 cm^{-1}, marked BeCCD, shifted only 6.1 cm^{-1} from its hydrogen counterpart in Figure 2a while the DBeCCD band at 781.9 cm^{-1} shifted in excess of 50 cm^{-1}. Trace C_2H_2 bands were present in the spectrum along with BeH_2 at 696.8 cm^{-1} and HCCD at 683.4 cm^{-1} (note the spectrum is expanded ×3 on the absorbance scale). The lowest product absorption in Figure 3c with sites at 451.3 and 450.0 cm^{-1} shifted in excess of 100 cm^{-1} and is marked DBeCCD.

Be + CH_3C_2H. Two experiments were done with beryllium and propyne under the same conditions employed for acetylene. Weak bands were observed for BeH_2 and $(BeO)_2$ as before. A trio of new bands was observed at 2038.9, 2033.6, and 2028.0 cm^{-1} (A = 0.03) in addition to sharp, weaker bands at 2159.4 (BeH_2) and 2112.9 cm^{-1} and a new band at 2019.0 cm^{-1} (A = 0.01). No 2119-cm^{-1} absorption was observed.

^{n}Mg + C_2H_2. Similar experiments were carried out reacting laser-ablated magnesium atoms with C_2H_2. Since product yields in magnesium experiments were lower, longer deposition periods were required. As with beryllium experiments the upper regions contained C_2H_2 bands at 3301.9 and 3288.4 cm^{-1} and C_4H_2 at 3325.9 cm^{-1}. In addition a very weak C_3 band was detected at 2039.0 cm^{-1} and CCH was observed at 1845.8 cm^{-1}.[29,30] Product absorptions for magnesium−acetylene reactions are listed in Table 2; no new magnesium−acetylene products were observed in the C−H stretching region.

Table 2. Absorptions (cm^{-1}) for Mg + HCCH Reaction Products in Solid Argon

assign	HCCH ^{24}Mg	H^{13}C^{13}CH ^{24}Mg	DCCD ^{24}Mg	HCCH ^{24}Mg	^{12}C/^{13}C ratios obsd	calcd^{a}
(site)	1982.7	1911.4	1854.7	1982.9	1.037303	1.037254
MgCCH	1984.2	1913.0	1856.4	1984.1	1.037219	1.037254
CCH	1845.8	1785.5	1746.9	1845.8	1.033772	1.036736
MgH	1421.9	1421.9		1419.5		
C_2H_2	736.7	734.9	542.5	736.7	1.002449	1.003051
MgCCH	660.8	656.2		660.8	1.007010	1.008659
MgCCH	491.8	482.0	485.1	482.8	1.020332	1.018639

^{a} Calculated by DFT, Table 8.

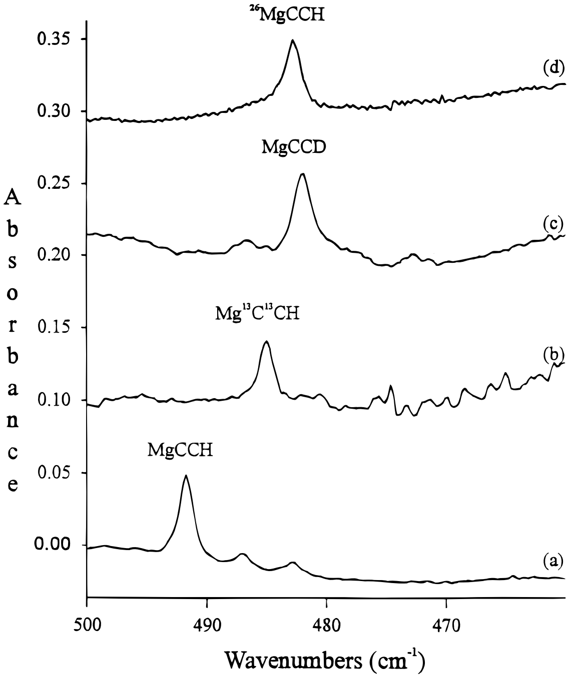

Figure 4. Infrared spectra from 500 to 460 cm^{-1} for Mg + C_2H_2 reaction products in solid argon at 10 ± 1 K: (a) ^{n}Mg + C_2H_2, (b) ^{n}Mg + $^{13}C_2H_2$, (c) ^{n}Mg + C_2D_2, and (d) ^{26}Mg + C_2H_2. Codeposition of Mg, 50 mJ/pulse, and Ar/C_2H_2 = 200/1 samples for 4 h.

Several Ar/C_2H_2 blank experiments assisted in the identification of a weak new band in the C−C stretching region. Sharp bands at 1972.1 and 1968.9 cm^{-1} are attributed to $(C_2H_2)_x$.[24] In addition two weak new bands at 1982.7 and 1984.2 cm^{-1} were detected. The radicals CCH and MgH were observed at 1845.8 and 1421.9 cm^{-1}, respectively.[26−29,31] In addition, a broad band at 660.8 cm^{-1} adjacent to CO_2, not present in acetylene samples, shifted with acetylene and magnesium isotopes, and is due to a product absorption. Diacetylene was again observed at 628.1 cm^{-1}.[25]

The region expected for Mg−C stretching modes also contained a strong new absorption; Figure 4a shows a sharp band at 491.8 cm^{-1} marked MgCCH. Note also the weaker bands at 487.0 and 482.8 cm^{-1}, which are of appropriate relative intensity (8/1/1) to be due to the ^{25}Mg and ^{26}Mg isotopes in natural abundance.

Mg + $^{13}C_2H_2$. Reactions of Mg with isotopic acetylene were carried out. With $^{13}C_2H_2$ a weak band for $^{13}C_3$ was observed at 1961.3 cm^{-1}.[29] In addition, weak new bands were present at 1911.4 and 1913.0 cm^{-1}. The band at 660.8 cm^{-1} with C_2H_2 shifted to 656.2 cm^{-1} with $^{13}C_2H_2$ samples. Finally, the band in the lower region in Figure 4b shifted to 482.0 cm^{-1} (marked Mg^{13}C^{13}CH).

Mg + C_2D_2. A Mg + C_2D_2 experiment revealed two weak absorptions at 1856.4 and 1854.7 cm^{-1} and a CCD radical at

---

(29) Weltner, W., Jr.; Walsh, P. N.; Angell, C. L. *J. Chem. Phys.* **1964**, *40*, 1299.

(30) Jacox, M. E.; Milligan, D. E. *Chem. Phys.* **1974**, *4*, 45.

(31) Tague, T. J., Jr.; Andrews, L. *J. Phys. Chem.* **1994**, *98*, 8611.

Table 3. Energies (au) for Be + HCCH and Mg + C_2H_2 Reaction Products Calculated Using Becke's Hybrid DFT Method with the Lee, Yang, Parr Functional (B3LYP) and 6-311G* Basis Sets

atom/molecule	symmetry, state	energy (au)
H	^2S	−0.502 156
H_2	$D_{\infty h}$, $^1\Sigma_g$	−1.176 632
Be	^3P	−14.580 757
Be	^1S	−14.671 184
BeH	$C_{\infty v}$, $^2\Sigma$	−15.264 396
CH	$C_{\infty v}$, $^4\Sigma$	−38.457 060
CH	$C_{\infty v}$, $^2\Sigma$	−38.490 299
CCH	$C_{\infty v}$, $^2\Sigma$	−76.626 486
CCH^-	$C_{\infty v}$, $^1\Sigma$	−76.722 749
CCH_2	C_{2v}, $^3B_2$	−77.206 927
CCH_2	C_{2v}, $^1A_1$	−77.281 150
HCCH	$D_{\infty h}$, $^1\Sigma_g$	−77.348 605
BeCCH	C_s, $^4A'$	−91.325 685
BeCCH	$C_{\infty v}$, $^2\Sigma$	−91.462 457
HBeCCH	C_s, $^3A'$	−91.979 737
$BeCCH_2$	C_{2v} branched, $^1A_1$	−91.99 249
$Be-C_2H_2$	C_{2v} ring, $^3B_2$	−92.031 775
$BeCCH_2$	C_{2v} branched, $^3B_2$	−92.041 719
$Be-C_2H_2$	C_{2v} ring, $^1A_1$	−92.064 345
HBeCCH	$C_{\infty v}$, $^1\Sigma$	−92.119 622
Mg	^3P	−199.990 786
Mg	^1S	−200.093 099
MgH	$C_{\infty v}$, $^2\Sigma$	−200.646 954
MgCCH	$C_{\infty v}$, $^2\Sigma$	−276.835 305
$Mg-C_2H_2$	C_{2v} ring, $^1A_1$	−277.378 882
$Mg-C_2H_2$	C_{2v} ring, $^3B_2$	−277.402 793
HMgCCH	$C_{\infty v}$, $^1\Sigma$	−277.453 954

1746.9 cm^{-1}. The new band in the magnesium−carbon stretching region shown in Figure 4c shifted to 485.1 cm^{-1} (marked MgCCD).

$^{26}Mg + C_2H_2$. In contrast to beryllium, another magnesium isotope, ^{26}Mg, is available to assist in the identification of product bands. Careful inspection revealed a small shift of the product in the C−C stretching region to 1982.6 and 1984.1 cm^{-1}. Similarly, the band in the magnesium−carbon stretching region, Figure 4d, shifted to 482.8 cm^{-1} (marked $^{26}MgCCH$), and is in agreement with the lower weak band observed with natural isotopic magnesium.

Quantum Chemical Calculations. A number of possible products were considered for the beryllium−acetylene and magnesium−acetylene systems. All calculations presented here were conducted on a Cray C90 Supercomputer at the San Diego Supercomputer Center using Gaussian 94.[32] Geometry optimizations and frequency calculations used Becke's Three Parameter Hybrid Density Functional Method with the Lee Yang Parr functional (collectively abbreviated B3LYP)[33] and 6-311G* basis sets for all atoms. Calculations on open-shell systems were unrestricted. Values for $\langle S^2 \rangle$ are provided and indicate negligible artificial spin contamination in these calculations.

Table 3 lists the optimized energies for several possible products. Calculations on different electronic states were performed to ensure that the ground electronic state was identified. The relative stability of beryllium−acetylene and magnesium−acetylene compounds has been studied extensively by Flores and Largo using complete second- and fourth-order Møller−Plesset levels of theory (MP2 and MP4).[20] In addition, Hartree−Fock SCF frequency calculations for natural abundance isotopes of each molecule in general are slightly higher than the B3LYP frequencies provided here, which are in turn slightly higher than the observed values. However, frequency and intensity calculations with isotopic substitution of carbon−13, deuterium, and magnesium-26 were not reported and these important calculations are provided here. Several starting geometries were considered for the optimization routines. Bent variations of HBeCCH and HMgCCH were considered; however, these converged to the linear structure.

Table 4. Frequencies (cm^{-1}), Bond Lengths (Å), and Bond Angles (deg) of HBeCCH, HCCH, and BeH Calculated Using B3LYP and 6-311G* Basis Sets

HBeCCH ($C_{\infty v}$, $^1\Sigma$)
$R_{Be-H} = 1.324$ $R_{Be-C} = 1.630$ $R_{C-C} = 1.214$
$R_{C-H} = 1.066$

	ω (*I*, km/mol)		
	HBeCCH	$HBe^{13}C^{13}CH$	DBeCCD
σ (C−H)	3446.1 (16)	3427.9 (18)	2674.2 (1)
σ (Be−H)	2191.0 (314)	2184.4 (277)	1639.6 (143)
σ (C−C)	2102.2 (15)	2033.3 (44)	1980.8 (152)
σ (Be−C)	859.0 (83)	849.8 (81)	807.8 (59)
π	703.2 (2 × 53)	696.6 (2 × 57)	558.1 (2 × 218)
π	587.9 (2 × 218)	585.9 (2 × 213)	486.3 (2 × 164)
π	221.5 (2 × 1)	215.7 (2 × 1)	194.1 (2 × 0)

HCCH ($D_{\infty h}$, $^1\Sigma_g$)
$R_{C-H} = 1.065$ $R_{C-C} = 1.199$

	ω (*I*, km/mol)		
	HCCH	$H^{13}C^{13}CH$	DCCD
σ_g	3512.8 (0)	3486.5 (0)	2814.7 (0)
σ_u	3410.0 (69)	3399.8 (69)	2503.7 (37)
σ_g	2067.8 (0)	2001.4 (0)	1825.5 (0)
π_u	756.1 (2 × 101)	753.8 (2 × 101)	555.1 (2 × 55)
π_g	560.8 (0)	552.3 (0)	468.0 (2 × 0)

BeH ($C_{\infty v}$, $^2\Sigma$) $\langle S^2 \rangle = 0.7512$
$R_{Be-H} = 1.3461$

	ω (*I*, km/mol)	
	BeH	BeD
σ	2045.6 (136)	1518.0 (75)

The stability orders for the beryllium−acetylene and magnesium−acetylene systems were the same as those reported by Flores and Largo.[20] For both systems the most stable ground state species was HMCCH ($^1\Sigma^+$). The stability order for the beryllium system using B3LYP is as follows: HBeCCH ($^1\Sigma^+$) > cyclic BeC_2H_2 ($^1A_1$) > $BeCCH_2$ ($^3B_2$) ∼ cyclic BeC_2H_2 ($^3B_2$) > $BeCCH_2$ ($^1A_1$) > HBeCCH ($^3A'$). Comparison of calculated frequencies provided in Tables 4−6 demonstrates that although linear BeCCH and HBeCCH have similar absorptions, the cyclic and vinylidene $Be-C_2H_2$ species are significantly different.

Several theoretical investigations on MgC_2H_2 species are also in the literature; MP2 and MP4 studies reported by Flores and Largo again resemble results presented here, as do SCF and CI calculations by Chaquin et al.[34] and Balaja and Jordan.[19b] The linear MgCCH radical was also investigated and isotopic frequencies are listed in Table 8.

Figure 5 shows B3LYP optimized structures for ground state beryllium−acetylene and magnesium−acetylene species. Comparisons of structures demonstrate that, as expected, Mg−C bonds are consistently longer than Be−C bonds in analogous

---

(32) Frisch, M. J.; Trucks, G. W.; Schlegel, H. B.; Gill, P. M. W.; Johnson, B. G.; Robb, M. A.; Cheeseman, J. R.; Keith, T.; Petersson, G. A.; Montgomery, J. A.; Raghavachari, K.; Al-Laham, M. A.; Zakrzewski, V. G.; Ortiz, J. V.; Foresman, J. B.; Cioslowski, J.; Stefanov, B. B.; Nanayakkara, A.; Challacombe, M.; Peng, C. Y.;Ayala, P. Y.; Chen, W.; Wong, M. W.; Andres, J. L.; Replogle, E. S.; Gomperts, R.; Martin, R. L.; Fox, D. J.; Binkley, J. S.; Defrees, D. J.; Baker, J.; Stewart, J. P.; Head-Gordon, M.; Gonzalez, C.; Pople J. A. *Gaussian 92 and Gaussian 94, Revision B.1.*; Gaussian, Inc.: Pittsburgh PA, 1995.

(33) Lee, C.; Yang, W.; Parr, R. G. *Phys. Rev. B* **1988**, *37*, 785. Becke, A. D. *J. Chem. Phys.* **1993**, *98*, 5648.

(34) Chaquin, P.; Sevin, A.; Papakondylis, A. *Chem. Phys.* **1990**, *143*, 39.

Table 5. Frequencies (cm^{-1}), Bond Lengths (Å), and Bond Angles (deg) of BeCCH, CCH, and CCH$^-$ Calculated Using B3LYP and 6−311G* Basis Sets

BeCCH ($C_{\infty v}$, $^2\Sigma$) $\langle S^2 \rangle = 0.7508$

$R_{\mathrm{Be-C}} = 1.635$ $R_{\mathrm{C-C}} = 1.215$ $R_{\mathrm{C-}} = 1.067$

	ω (*I*, km/mol)		
	BeCCH	Be^{13}C^{13}CH	BeCCD
σ (C−H)	3442.8 (16)	3424.6 (18)	2670.3 (0)
σ (C−C)	2108.1 (115)	2033.0 (107)	1969.0 (120)
σ(Be−C)	877.7 (123)	869.0 (120)	869.7 (117)
π	708.5 (2 × 43)	701.7 (2 × 44)	561.9 (2 × 21)
π	240.7 (2 × 5)	234.0 (2 × 4)	228.7 (2 × 5)

CCH ($C_{\infty v}$, $^2\Sigma$) $\langle S^2 \rangle = 0.7503$

$R_{\mathrm{C-C}} = 1.201$ $R_{\mathrm{C-H}} = 1.066$

	ω (*I*, km/mol)		
	CCH	^{13}C^{13}CH	CCD
σ (C−H)	3451.0 (45)	3432.3 (45)	2682.2 (15)
σ (C−C)	2088.38 (6)	2014.4 (5)	1939.0 (11)
π	229.1 (2 × 4)	226.8 (2 × 4)	182.2 (2 × 4)

CCH$^-$ ($C_{\infty v}$, $^1\Sigma$)

$R_{\mathrm{C-C}} = 1.2042$ $R_{\mathrm{C-H}} = 1.0732$

	ω (*I*, km/mol)		
	CCH	^{13}C^{13}CH	CCD
σ(C−H)	3323.4 (14)	3306.6 (16)	2554.9 (0)
σ(C−C)	1898.2 (136)	1829.9 (33)	1781.4 (30)
π	513.9 (2 × 51)	508.7 (61)	408.1 (31)

Table 6. Frequencies (cm^{-1}), Bond Lengths (Å), and Bond Angles (deg) of Cyclic Be−C$_2$H$_2$ and BeCCH$_2$ Calculated Using B3LYP and 6−311G* Basis Sets

Be−C$_2$H$_2$ (C_{2v}, ^{1}A$_1$)

$R_{\mathrm{BeC}} = 1.556$ $R_{\mathrm{CC}} = 1.388$ $R_{\mathrm{CH}} = 1.088$

∠BeCH = 170.5 ∠CBeC = 53.0

	ω (*I*, km/mol)		
	Be−C$_2$H$_2$	Be−^{13}C$_2$H$_2$	BeC$_2$D$_2$
A$_1$	3148.8 (37)	3137.3 (36)	2347.2 (18)
B$_2$	3127.7 (32)	3117.4 (33)	2312.1 (9)
A$_1$	1407.4 (0)	1366.3 (0)	1362.2 (0)
B$_2$	1169.0 (5)	1147.5 (4)	1061.4 (111)
A$_1$	1063.1 (104)	1044.2 (98)	1051.3 (25)
A$_2$	1023.2 (0)	1013.8 (0)	804.8 (0)
B$_2$	923.5 (54)	912.2 (54)	784.0 (33)
A$_1$	906.1 (22)	702.9 (126)	647.3 (9)
B$_1$	707.6 (129)	905.1 (24)	557.0 (93)

BeCCH$_2$ (C_{2v}, ^{3}B$_2$) $\langle S^2 \rangle = 2.009$

$R_{\mathrm{Be-C}} = 1.491$ $R_{\mathrm{C-C}} = 1.321$ $R_{\mathrm{C-H}} = 1.095$

∠CCH = 122.9

	ω (*I*, km/mol)		
	BeCCH$_2$	Be^{13}C^{13}CH$_2$	BeCCD$_2$
B$_2$	3090.4 (7)	2295.3 (5)	2295.3 (5)
A$_1$	3039.5 (15)	2222.0 (12)	2222.0 (12)
A$_1$	1749.3 (37)	1713.7 (37)	1713.7 (37)
A$_1$	1410.8 (18)	1057.9 (36)	1057.9 (36)
B$_2$	928.6 (0)	824.1 (64)	824.1 (64)
B$_1$	919.7 (46)	750.1 (2)	750.1 (2)
A$_1$	860.1 (88)	736.0 (25)	736.0 (24)
B$_1$	256.0 (1)	249.6 (1)	249.6 (1)
B$_2$	246.1 (6)	225.7 (4)	225.7 (4)

species. Bond lengths and angles are also provided in Tables 4−8 along with isotopic frequency calculations, which are discussed with product assignments in the following section.

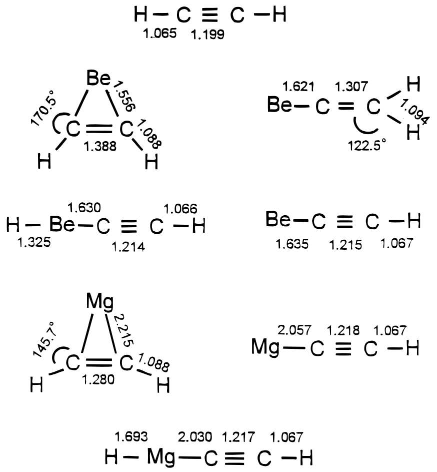

Figure 5. Bond lengths (Å) and angles (deg) for stable isomers of possible beryllium−acetylene and magnesium−acetylene reaction products calculated at the B3LYP level with 6-311G* basis sets.

Table 7. Frequencies (cm^{-1}), Bond Lengths (Å), and Bond Angles (deg) of HMgCCH and MgH Calculated Using B3LYP and 6−311G* Basis Sets

HMgCCH ($C_{\infty v}$, $^1\Sigma$)

$R_{\mathrm{Mg-H}} = 1.693$ $R_{\mathrm{Mg-C}} = 2.030$ $R_{\mathrm{C-C}} = 1.217$

$R_{\mathrm{C-H}} = 1.067$

	ω (*I*, km/mol)		
	HMgCCH	HMg^{13}C^{13}CH	DMgCCD
σ (C−H)	3434.3 (15)	3416.3 (16)	2658.1 (2)
σ (C−C)	2066.9 (34)	1992.7 (31)	1930.6 (40)
σ(Mg−H)	1667.1 (212)	1667.0 (212)	1205.0 (132)
π	671.1 (2 × 62)	665.4 (2 × 63)	525.5 (2 × 25)
σ(Mg−C)	514.4 (65)	504.9 (62)	502.4 (58)
π	369.0 (2 × 304)	367.6 (2 × 300)	289.8 (2 × 193)
π	144.9 (2 × 1)	140.6 (2 × 1)	129.8 (2 × 0)

	ω (*I*, km/mol)		
	H^{26}MgCCH	H^{26}Mg^{13}C^{13}CH	D^{26}MgCCD
σ (C−H)	3434.3 (15)	3416.3 (16)	3416.3 (16)
σ (C−C)	2066.8 (33)	1992.6 (31)	1992.6 (31)
σ(Mg−H)	1664.4 (209)	1664.4 (208)	1664.4 (208)
π	671.1 (2 × 62)	665.4 (2 × 63)	665.4 (2 × 63)
σ(Mg−C)	504.9 (63)	495.1 (60)	495.1 (60)
π	367.1 (2 × 301)	365.8 (2 × 298)	365.8 (2 × 298)
π	144.8 (2 × 1)	140.5 (2 × 1)	140.5 (2 × 1)

MgH ($C_{\infty v}$, $^2\Sigma$) $\langle S^2 \rangle = 0.7549$

$R_{\mathrm{Mg-H}} = 1.7528$

	ω (*I*, km/mol)		
	MgH	MgD	^{26}MgH
σ	1439.0 (241)	1038.2 (126)	1436.7 (241)

Discussion

Product band assignments and reaction mechanisms will be presented.

HBeCCH. The diagnostic band for the HBeCCH group is the site-split doublet of bands at 553.0 and 550.0 cm^{-1}; this band shows large deuterium and small ^{13}C isotope shifts and appears in the region expected for the HBeC bending mode. The insertion product, HBeCCH, is a likely candidate since previous studies with laser-ablated beryllium suggest that metastable Be atoms undergo insertion reactions.[14,16,35] In fact the observed bands are in excellent agreement with the

---

(35) Andrews, L.; Chertihin, G.; Thompson, C. A.; Dillon, J.; Byrne, S.; Bauschlicher, C. W., Jr. *J. Phys. Chem.* **1996**, *100*, 10088.

Table 8. Frequencies (cm^{-1}), Bond Lengths (Å), and Bond Angles (deg) of MgCCH Calculated Using B3LYP and 6−311G* Basis Sets

	MgCCH	($C_{\infty v}$, $^2\Sigma$)	$\langle S^2 \rangle = 0.751$
	$R_{MgC} = 2.057$	$R_{C-C} = 1.218$	$R_{C-H} = 1.067$
	ω (I, km/mol)		
	MgCCH	$Mg^{13}C^{13}CH$	MgCCD
σ(C−H)	3432.6 (15)	3414.7 (15)	2654.5 (3)
σ(C−C)	2054.8 (23)	1981.0 (21)	1920.4(31)
π	664.0 (2 × 48)	658.3 (2 × 48)	520.2 (2 × 24)
σ(Mg−C)	486.4 (87)	477.5 (84)	480.9 (85)
π	136.1 (2 × 13)	131.7 (2 × 12)	129.3 (2 × 13)
	ω (I, km/mol)		
	$^{26}MgCCH$	$^{26}Mg^{13}C^{13}CH$	$^{26}MgCCD$
σ(C−H)	3432.6 (15)	3414.6 (15)	2654.5 (3)
σ (C−C)	2054.7 (23)	1980.9 (2 × 21)	1920.3 (31)
π	664.0 (2 × 48)	658.3 (2 × 48)	520.1 (2 × 24)
σ(Mg−C)	476.7 (84)	467.7 (81)	471.2 (82)
π	135.8 (2 × 13)	131.4 (2 × 12)	129.0 (2 × 12)

calculated absorptions for HBeCCH presented in Table 4; other molecules lacking the HBeC subunit are not expected to have bands in the 550-cm^{-1} region. The molecule HBeCCH also has an intense Be-H stretching mode blue-shifted about 150 cm^{-1} from the calculated BeH fundamental. Note that the HBeCCH band in Figure 2a is blue-shifted 149 cm^{-1} from the BeH fundamental observed by Tague and Andrews[15] at 1970.1 cm^{-1}; BeH was also observed in these experiments in low yield. Calculations also predict the Be−H stretching mode of $HBe^{13}C^{13}CH$ to be red-shifted 6.6 cm^{-1} from HBeCCH. The observed value of 4.2 cm^{-1} is in good agreement when considering the complex description of the mode arising from mixing with the C−C stretch, as indicated by an increase in intensity for the C−C stretch of $HBe^{13}C^{13}CH$ relative to HBeCCH. In addition, the observed deuterium shift of 584.4 cm^{-1} is in good agreement with the predicted value of 551.4 cm^{-1} considering anharmonicity, which is not accounted for in the B3LYP harmonic frequency calculations.

Excellent agreement between the calculated and observed isotopic frequencies for Be−C stretching modes and CCH bending modes of HBeCCH is also found here. The upper band marked HBeCCH (Figure 3) corresponds to the Be−C stretching mode. Note that the ^{13}C counterpart band appeared 9.3 cm^{-1} red-shifted in excellent agreement with the BeC stretch of HBeCCH (859.0 cm^{-1}), which has a 9.2 cm^{-1} calculated ^{13}C shift. The observed deuterium shift of 54.0 cm^{-1} is also in excellent agreement with the calculated deuterium shift of 51.2 cm^{-1}. Similarly, the broad 689.1-cm^{-1} band of Figure 3 agrees well with the CCH bend calculated at 703.2 cm^{-1}. The band shifts 5.8 cm^{-1} with ^{13}C compared to a calculated shift of 6.6 cm^{-1}. Upon deuterium substitution the band shifted 128.2 cm^{-1} compared to the calculated shift of 145.1 cm^{-1}.

The excellent agreement between calculated and observed frequencies for the most intense absorptions strongly supports assignment of these bands to HBeCCH, a linear molecule observed here for the first time. Andrews et al. identified the C−C stretch of the similar HBCCH molecule formed by reaction of laser-ablated boron with acetylene.[9] In addition Burkholder and Andrews observed HAlCCH from the photolysis of aluminum−acetylene complexes.[7] Both HBCCH and HAlCCH are expected to be bent and have substantially different M−H stretching modes as well as HMC bending modes. Unfortunately, the C−C stretching mode for HBeCCH is calculated to be weak, and this mode is not observed here. Based on energy calculations the linear HBeCCH molecule is the most stable BeC_2H_2 structural isomer and the only one observed in these experiments.

BeCCH. Several bands in the product spectra were adjacent to HBeCCH absorptions implying a similar chemical species with similar vibrational modes. Note the band marked BeCCH at 855.0 cm^{-1} is 16.1 cm^{-1} above the Be−C stretch of HBeCCH (Figure 2). The band shifted 8.8 cm^{-1} to the red upon ^{13}C substitution; however, it only shifted 6.1 cm^{-1} with D substitution compared to 54.0 cm^{-1} for the Be−C stretch of HBeCCH, indicating that the molecule has a similar Be−C stretching mode with much less hydrogen interaction. These shifts are in excellent agreement with isotopic frequency calculations for linear BeCCH presented in Table 5; the Be−C stretching mode of $Be^{13}C^{13}C$ is calculated to red shift 8.7 cm^{-1} from $Be^{12}C^{12}CH$ and the observed shift is 8.8 cm^{-1}! A comparison can also be made of the relative Be−C stretching frequencies of HBeCCH and BeCCH. As shown in Tables 4 and 5, BeCCH is calculated to have a Be−C stretching mode 18.7 cm^{-1} higher than HBeCCH, in agreement with the observed difference of 15.1 cm^{-1}.

The molecule BeCCH is calculated to have a CCH bending mode at 708.5 cm^{-1}, slightly higher than the analogous mode of HBeCCH. The observed band at 675.7 cm^{-1} is actually red-shifted 13.4 cm^{-1}; however, this discrepancy is attributed to the more complex description for the bending mode of the BeCCH radical. The C−C stretching mode of BeCCH was observed at 2018.9 cm^{-1} compared with the calculated frequency of 2108.1 cm^{-1}. Using the C−C stretching fundamental of acetylene from the Raman spectrum (1974 cm^{-1}),[36] a comparison of the observed/calculated ratio for the C−C stretch of acetylene (0.955) can be made to the observed/calculated ratio for the C−C stretch of HBeCCH (0.958). The almost equal ratios indicate excellent agreement between the calculated and observed spectra. Note that although HBeCCH and BeCCH are calculated to have C−C stretching modes within 6 cm^{-1} of each other, the C−C stretching mode of BeCCH is calculated to be seven times greater intensity. Accordingly the failure to observe the C−C stretching mode of HBeCCH is attributed to low intensity. For BeCCH the calculated and observed isotope shifts are in very good agreement: ^{13}C (75.1 cm^{-1} calculated, 71.8 cm^{-1} observed) and deuterium (139.1 cm^{-1} calculated, 145.5 cm^{-1} observed).

The observation of the Be−C stretching mode significantly less coupled to hydrogen, relative to HBeCCH, and general agreement of the observed and calculated isotopic frequencies strongly supports identification of the new linear $^2\Sigma$ BeCCH radical, which is isoelectronic to the Mg, Ca, and Sr acetylide radicals reported earlier.[10,11] Comparison of the C−C stretch of CCH^- (1800 cm^{-1} in solid neon)[37] reveals, as expected, a lower C−C frequency for the anion species. Calculations presented in Table 4 predict the C−C stretching vibration of BeCCH to be 210 cm^{-1} to the blue of the C-C stretch of CCH^-, in agreement with the observed difference of 219 cm^{-1}. The analogous BCCH and AlCCH molecules have also been produced by laser-ablated B and Al reactions with C_2H_2.[8,9] The C−C stretch for $^{11}BCCH$ (2039.3 cm^{-1}) is slightly to the blue of the C−C stretch of BeCCH (2018.9 cm^{-1}). In contrast, the C−C stretch of AlCCH (2000.8 cm^{-1}) is to red of BeCCH as is a tentative assignment to the C−C mode of MgCCH (1984.2 cm^{-1}), which will be discussed in the following section.

$BeCCCH_3$. The Be atom reaction with propyne followed the reaction with acetylene. Weak bands were observed for BeH_2

---

[36] Herzberg, G. *Infrared and Raman Spectra of Polyatomic Molecules*; D. Van Nostrand Co. Inc.: New York, 1945.

[37] Forney, D.; Jacox, M. E.; Thompson, W. E. *J. Mol. Spectrosc.* **1992**, *153*, 680.

at 2159.4 cm^{-1} and BeCCH at 2019.0 cm^{-1}. The major product gave 3 site split bands at 2038.9, 2033.6, and 2028.0 cm^{-1}, which is assigned to the methyl-substituted BeCCCH$_3$ radical. The small blue shift in the C≡C fundamental on methyl substitution follows the trend for propyne.[24] The weak, sharp 2112.9-cm^{-1} band is tentatively assigned to the Be−H stretching mode in HBeCCCH$_3$; note that HBeCCH was absent in propyne experiments but BeCCH was observed.

MgCCH. Product band intensities in Mg + HCCH experiments suffered from two effects: laser-ablated Mg is generally less reactive than Be resulting in decreased product yield,[14,38] and calculated intensities for the product molecules are less for MgCCH than for BeCCH. The most distinguishing feature in the magnesium experiments is the strong band at 491.8 cm^{-1} in the Mg−C stretching region (Figure 4). It is important to consider the 8/1/1 triplet for this band using natural ^{24}Mg, ^{25}Mg, and ^{26}Mg isotopic magnesium (Figure 4a). Agreement of the ^{26}Mg band with the enriched ^{26}Mg reaction product (Figure 4d) confirms the presence of a single Mg atom in this molecule. Calculations for $^3B_2$ Mg−C$_2$H$_2$ predict a small (2.4 cm^{-1}) carbon−13 and a large (77 cm^{-1}) deuterium shift for the strong 506-cm^{-1} Mg−C$_2$ stretching fundamental[39] which is clearly not in accord with the 491.8-cm^{-1} band observed here. Note that the observed Mg−C stretching frequency is within the range calculated for both MgCCH and HMgCCH (Tables 7 and 8). However, the strongest observable band for HMgCCH is the Mg−H stretching mode calculated at 1667.1 cm^{-1}, but such a band was not detected in the present experiments indicating that the observed Mg−C stretching band probably belongs to MgCCH.

Furthermore, the 491.8-cm^{-1} band in Figure 4 is in better agreement with the Mg−C stretching mode calculated for MgCCH (486.4 cm^{-1}) than for HMgCCH (514.4 cm^{-1}). The calculated and observed isotope shifts for ^{13}C (8.9 cm^{-1} calculated, 9.8 cm^{-1} observed), D (5.5 cm^{-1} calculated, 6.7 cm^{-1} observed), and ^{26}Mg (9.7 cm^{-1} calculated, 9.0 cm^{-1} observed) are in excellent agreement for MgCCH. In contrast, the D shift for DMgCCD is calculated to be larger (12.0 cm^{-1}) as expected. In addition, the band at 660.8 cm^{-1} is in agreement with the CCH bend of MgCCH calculated at 664.0 cm^{-1}. The ^{13}C counterpart band shifted 4.6 cm^{-1} to the red in reasonable agreement with the calculated shift of 5.7 cm^{-1}.

The observation of a Mg−C stretching mode at 491.8 cm^{-1} and a CCH bending mode at 660.8 cm^{-1} along with the absence of the strong Mg−H stretching absorption are sufficient to assign observed bands to MgCCH. Weak matrix site bands at 1982.7 and 1984.2 cm^{-1} are tentatively assigned to the C−C stretching mode of MgCCH; this mode is below the C−C stretch of AlCCH (2000.8 cm^{-1}). This trend agrees with the trend observed for the C−C stretch of BeCCH, which is red-shifted from BCCH by 20.4 cm^{-1}.

The 491.8-cm^{-1} matrix value for the Mg−C stretching mode in MgCCH is in excellent agreement with a preliminary 500 ± 5 cm^{-1} value deduced from the emission spectrum of the gaseous species[11c] allowing for a small red shift by the argon matrix. The trend in M−C stretching frequencies and "diatomic" stretching force constants calculated for M−CCH molecules from Be (855 cm^{-1}, $k_{\mathrm{Be-C}} = 2.22$ mdyn/Å) and Mg (492 cm^{-1}, $k_{\mathrm{Mg-C}} = 1.14$ mdyn/Å) to Ca (399 cm^{-1}, $k_{\mathrm{Ca-C}} = 0.87$ mdyn/Å)[10a] and Sr (343 cm^{-1}, $k_{\mathrm{Sr-C}} = 0.73$ mdyn/Å)[10a] reinforces these assignments. Note that the Mg−C force constant is slightly higher than Ca−C and Sr−C values but substantially lower than the "diatomic" Be−C force constant.

Reaction Mechanisms. Previous experiments involving laser-ablated beryllium and magnesium have shown atomic Be and Mg to be reactive species.[14,38] Metastable Mg($^3P_1$) has a lifetime of 2−4 ms[40] and is likely the reactive species in magnesium experiments.[38] Similarly, Be($^3P_1$) is the probable reactant here since the lifetime of metastable Be is expected to be longer owing to less spin−orbit coupling. The primary reaction of beryllium probably forms both major products:

$$\mathrm{Be^* + HCCH \rightarrow [HBeCCH]^* \xrightarrow{relax} HBeCCH} \qquad (\Delta E = -63\ \mathrm{kcal/mol}) \quad (1)$$

$$\xrightarrow{dec} \mathrm{H + BeCCH} \qquad (\Delta E = +35\ \mathrm{kcal/mol}) \quad (2)$$

The matrix can relax the energized insertion product or it can decompose. Using B3LYP calculated energies and starting with ground state Be, reaction 1 is expected to be exothermic by approximately 63 kcal/mol, while reaction 2 is endothermic by about 35 kcal/mol. Metastable Be($^3P_1$) is 61 kcal/mol higher in energy,[41] and if this energy is used, reactions 1 and 2 become exothermic by 124 and 26 kcal/mol, respectively. Reaction energetics calculated here are in agreement (±10 kcal/mol) with those of Flores and Largo using MP4 calculated energies.[20]

The presence of BeH, BeH$_2$, CCH, and HCCCCH, the dimer of the CCH radical, all indicate that some fraction of the beryllium atoms are in effect abstracting hydrogen from HCCH:

$$\mathrm{Be^* + HCCH \rightarrow BeH + CCH} \qquad (\Delta E = +81\ \mathrm{kcal/mol}) \quad (3)$$

This reaction is calculated to be endothermic by 81 kcal/mol using ground-state Be and endothermic by 20 kcal/mol using Be($^3P_1$). The obsevation of BeH and CCH in these experiments requires still more energy in the reacting Be atoms, and such excess kinetic energy is available in laser-ablated metal atoms.[14,42] The presence of CCH suggests a second possible pathway for formation of BeCCH from the simple exothermic combination reaction 4.

$$\mathrm{Be + CCH \rightarrow BeCCH} \qquad (\Delta E = -103\ \mathrm{kcal/mol}) \quad (4)$$

Finally, the combination of CCH radicals accounts for the formation of diacetylene:

$$\mathrm{HCC + CCH \rightarrow HCCCCH} \quad (5)$$

The insertion product HMgCCH was not found in the magnesium spectra; however, MgH and CCH were observed. This suggests that the insertion product is not relaxed but decomposes straightaway by reaction 6. Then MgCCH can be formed by the simple exothermic combination reaction 7.

$$\mathrm{Mg^* + HCCH \rightarrow [HMgCCH]^* \xrightarrow{dec} MgH + CCH} \qquad (\Delta E = +106\ \mathrm{kcal/mol}) \quad (6)$$

$$\mathrm{Mg + CCH \rightarrow MgCCH} \qquad (\Delta E = -73\ \mathrm{kcal/mol}) \quad (7)$$

Using ground state Mg, reaction 6 is calculated to be endothermic by 106 kcal/mol, while reaction 7 is calculated to be exothermic by 73 kcal/mol. Thermodynamic data for acetylene

---

[38] Andrews, L.; Yustein, J. T. *J. Phys. Chem.* **1993**, *97*, 12700.

[39] Thompson, C. A. Ph.D. Thesis, University of Virginia, Charlottesville, 1996.

[40] Husain, D. *J. Chem. Soc., Faraday. Trans.* **1989**, *85*, 85. Furcinitti, P. S.; Wright, J. J.; Balling, L. C. *Phys. Rev. A* **1975**, *12*, 1123

[41] Paschen, F.; Kruger, P. G. *Ann. Phys.* **1931**, *8*, 1005. Herzberg, G. *Atomic Spectra and Atomic Structure*; Dover Publications: New York, 1944.

[42] Wang, H.; Salzberg, A. P.; Weiner, B. R. *Appl. Phys. Lett.* **1991**, *59*, 935.

and MgH suggest that reaction 6 is endothermic by 84 ± 10 kcal/mol, which shows that the DFT energy calculation is too endothermic. Nevertheless, excess energy is required to promote reaction 6. Metastable Mg is 63 kcal/mol higher[40] than ground state Mg, and substantial excess kinetic energy is available in laser-ablated metal atoms as well.[38,42]

Another route for the formation of MgCCH, reaction 8, is

$$\mathrm{Mg^* + HCCH \rightarrow HMgCCH^* \rightarrow H + MgCCH} \qquad (\Delta E = +65\ \mathrm{kcal/mol}) \quad (8)$$

endothermic by 65 kcal/mol when calculated using ground state Mg and endothermic by only 2 kcal/mol using ^3P Mg. This shows that excess metal atom kinetic energy is necessary for these reactions to proceed and suggests that reaction 8 is the preferred pathway for the formation of MgCCH.

Conclusions

Products of laser ablated beryllium and magnesium reactions with acetylene included the organometallic molecules HBeCCH, BeCCH, and MgCCH as well as the BeH and MgH metal hydrides, the CCH radical, and its dimer diacetylene. The spectra suggest a mechanism involving the insertion of metastable excited metal atoms into the CH bond of acetylene followed by subsequent relaxation or decomposition. The observation of CCH in these reactions highlights the availability of energy for endothermic processes from laser ablated metal atoms which often results in the formation of products not seen with thermal atom reactions. Once formed CCH radical can combine straightaway with Be and Mg atoms. The failure to observe HMgCCH may be due to the weaker MgH bond as compared to the BeH bond.[43] Although ground state Be is unreactive, metastable ($^3P_1$) Be is reactive and once formed, the BeH bond is strong enough to be stable.

Laser ablated Be and propyne gave BeCCH and $BeCCCH_3$ with the latter ν(C≡C) mode blue-shifted 15 ± 5 cm^{-1} from the former value as is customary for methyl substituents.

The BeCCH and MgCCH molecules have Be−C and Mg−C stretching frequencies at 855 and 492 cm^{-1}, which characterize stable alkaline earth metal−carbon bonds. These frequencies are, of course, higher than the Ca−C (399 cm^{-1}) and Sr−C (343 cm^{-1}) values for the gaseous CaCCH and SrCCH molecules.[10a] The C−C stretching frequencies for BeCCH and MgCCH are slightly lower than values for BCCH and AlCCH, respectively, but somewhat higher than values for CCH and CCH^-.

Density functional theory was used to calculate structures and isotopic frequencies to provide efficient and valuable support for the experimental observation and identification of these new organometallic molecules.

Acknowledgment. We appreciate financial support from NSF Grant CHE 92−55662, computer time at the San Diego Supercomputer Center, and helpful correspondence with P. v. R. Schleyer.

JA9616847

---

[43] Huber, K. P.; Herzberg, G. *Constants of Diatomic Molecules*; Van Nostrand Reinhold: New York, 1979.